

## Optical properties of magnetic sawtooth superlattices

P. Harrison\*

*Department of Electronic and Electrical Engineering, University of Leeds, Leeds LS2 9JT, United Kingdom*

T. Piorek, T. Stirner, and W. E. Hagston

*Department of Applied Physics, University of Hull, Hull HU6 7RX, United Kingdom*

(Received 3 October 1995)

Self-consistent calculations of the optical properties of magnetic sawtooth superlattices are presented. Sawtooth modulation of the graded gap superlattice as produced by linear variations of the magnetic  $\text{Mn}^{2+}$  ion in the  $\text{Cd}_{1-x}\text{Mn}_x\text{Te}$  alloy is described. The Brillouin function response of the band gap together with the varying manganese concentration produces unusual potential profiles in an external magnetic field. The calculations show that the low-temperature magnetic field tunability of the exciton emission is greater in sawtooth superlattices than in an equivalent rectangular superlattice structure. A means of utilizing this for probing alloy nonrandomness is described.

### I. INTRODUCTION

Sawtooth superlattices where the band-gap modulation is produced by a linear variation of one of the constituents in an alloy, e.g., aluminum (Al) in  $\text{Ga}_{1-x}\text{Al}_x\text{As}$ , have attracted considerable attention in the literature.<sup>1-4</sup> However, very little work has been done on graded gap semiconductor superlattices where the band-gap modulation is produced by a linear variation of a magnetic ion in a diluted magnetic semiconductor.

The calculations presented here deal specifically with the situation where the superlattice has been created by varying the concentration of the magnetic ion  $\text{Mn}^{2+}$  in the diluted magnetic semiconductor  $\text{Cd}_{1-x}\text{Mn}_x\text{Te}$ . The conduction- and valence-band edges respond to an external magnetic field in the form of a modified Brillouin function, whose parameters vary in a known manner with the concentration of the  $\text{Mn}^{2+}$  ions. Since the latter varies linearly across the superlattice, the corresponding superlattice potential can be moved continuously through a series of novel potential profiles as the magnetic field is increased. The influence of these potential profiles on the exciton emission energies are evaluated.

### II. THEORY

The system investigated was produced by varying the manganese concentration  $x$  between two limits  $x_{\max}$  and  $x_{\min}$  in a linear fashion, as depicted in Fig. 1. A finite number ( $N$ ) of periods was considered with  $x$  varying so as to produce a symmetric sawtooth or "triangular" superlattice, i.e., in the following calculations the length  $a$  was always chosen to be equal to  $b$ . Similarly the minimum value of  $x$ , i.e.,  $x_{\min}$ , was taken to be zero, as this produced a convenient (field independent) reference point for the magnetic field investigations. Further, the maximum value of the manganese concentration  $x_{\max}$  was taken to be 0.075 (i.e., 7.5%).

Assuming the validity of the envelope function approximation,<sup>5</sup> the one-particle Hamiltonian can be written,

$$\mathcal{H}_z = -\frac{\hbar^2}{2m_z^*} \frac{\partial^2}{\partial z^2} + \mathcal{V}(z), \quad (1)$$

where  $m_z^*$  is the effective mass of the electron or hole and  $\mathcal{V}(z)$  is the conduction- (or valence-) band potential profile along the growth direction for the electron (or hole). The conduction-band profile for the electron, measured with respect to the bottom of the well, has the form<sup>6</sup>

$$\mathcal{V}(z) = (1 - \kappa)\xi x(z),$$

while the valence-band potential for the hole is given by

$$\mathcal{V}(z) = \kappa\xi x(z),$$

where  $\kappa$  represents the proportion of the total offset that lies in the valence band and  $\xi$  [=1587 meV (Ref. 6)] is the proportionality constant linking the change in band gap  $E_{\text{gap}}$  (note  $E_{\text{gap}}^{\text{CdTe}} = 1606$  meV) to the manganese concentration  $x(z)$ , i.e.,

$$E_{\text{gap}}^{\text{Cd}_{1-x}\text{Mn}_x\text{Te}} - E_{\text{gap}}^{\text{CdTe}} = \xi x.$$

The Schrödinger equation corresponding to the Hamiltonian of Eq. (1) was solved numerically using the shooting technique.<sup>7</sup> This method yields both the one-particle energies  $E_e$  and  $E_h$  and the uncorrelated eigenfunctions  $\psi_e$  and  $\psi_h$  of the electron and hole, respectively.

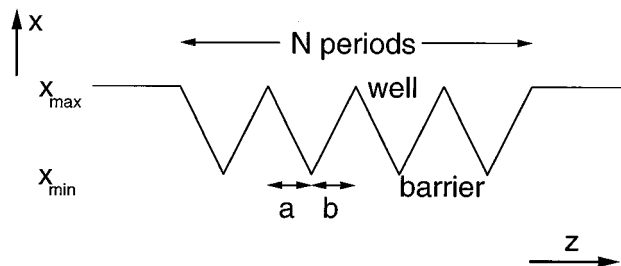


FIG. 1. Variation of the manganese concentration  $x$  in the symmetric finite sawtooth superlattice.

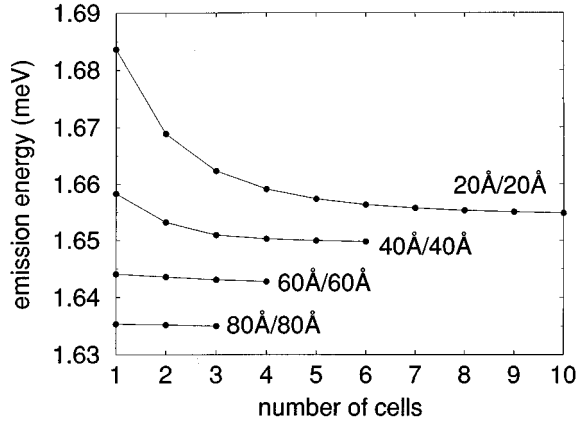


FIG. 2. Heavy-hole exciton emission energy as a function of the number of sawtooth superlattice periods for four different spatial parameters.

As only dilute alloys were considered the effective masses ( $m_e^*=0.096$  and  $m_{hh}^*=0.6$ ) and the relative permittivity [ $\epsilon=10.6$  from the three-dimensional Rydberg of 10 meV (Ref. 8)] were taken to be constant for the differing alloys. Similarly  $\kappa$  was chosen to be 0.4.<sup>9</sup>

The uncorrelated electron and hole eigenfunctions, i.e.,  $\psi_e$  and  $\psi_h$ , respectively, were used to calculate the exciton binding energy  $E_b$  appropriate to these energy levels, using the technique of Hilton *et al.*<sup>10,11</sup> These results were then used, in a similar manner to Warnock *et al.*,<sup>12</sup> as the basis for a self-consistent treatment of the problem.<sup>13</sup> For example, the first iterated form of the one-electron wave function is obtained from the solution of

$$\left[ \int \psi_h^* \psi_r^* \mathcal{H} \psi_h \psi_r dz_h dx_\perp dy_\perp \right] \psi_e(z_e) = E \left[ \int |\psi_h|^2 |\psi_r|^2 dz_h dx_\perp dy_\perp \right] \psi_e(z_e). \quad (2)$$

Given this new  $\psi_e(z_e)$  the indices in Eq. (2) can be interchanged to give an improved approximation for  $\psi_h(z_h)$ . With these two new single-particle wave functions the exciton binding energy variational calculation was invoked again until the energy  $E$  reached a new minimum. This iterative loop was repeated until the results converged.

### III. RESULTS AND DISCUSSION

The exciton energies as a function of the number of sawtooth unit cells are shown in Fig. 2 for four different well widths (delineated by  $a/b$ ). Figure 2 shows clearly that for the  $a=b=20$  Å sawtooth, the exciton energy decreases initially as the number of unit cells increases. This is due to the reduction in the quantum confinement energy of both the electron and hole resulting from the increasing width of the energy band accompanying the increasing delocalization of the wave function from the single well case. It can be seen from the graph that the exciton energy is constant to within 1 meV once the number of periods is greater than 9 or 10.

The sawtooths characterized by  $a=b$  equal to 40, 60 and 80 Å behave in a qualitatively similar manner, however,

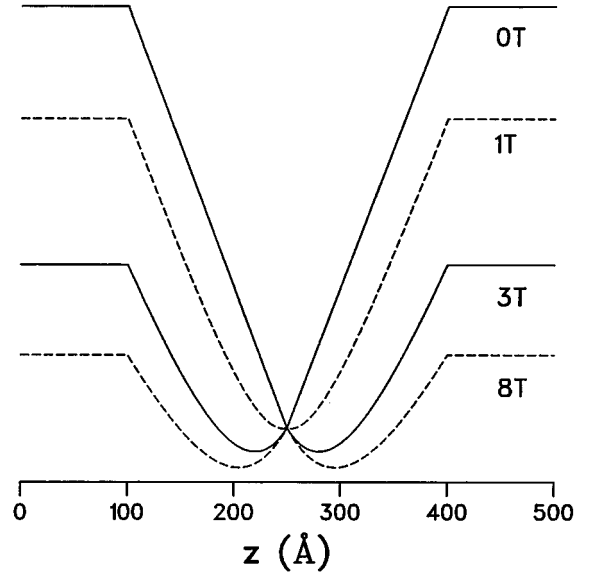


FIG. 3. Effect of magnetic field on the valence band ( $m_j = -\frac{3}{2}$ ) potential profile of a single sawtooth period for a 40% valence-band offset at a temperature of 1.8 K.

fewer periods are required as the thicker barriers inhibit the coupling between the wells.

As mentioned earlier, the uniqueness of the systems described here lies in the novel potential profile effects, which can be produced by the application of an external magnetic field along the superlattice direction. The band gap of the diluted magnetic semiconductor  $\text{Cd}_{1-x}\text{Mn}_x\text{Te}$  can be either increased or decreased with respect to CdTe depending on whether the  $\sigma^-$  or  $\sigma^+$  optical polarized transitions are observed.<sup>14</sup> The conduction-band edge of  $\text{Cd}_{1-x}\text{Mn}_x\text{Te}$  changes by an amount  $3A$  and the heavy-hole valence-band edge by an amount  $3B$  where

$$|A| = \frac{1}{6} x N_0 \alpha s_0(x) B_J(\mathbf{B}, x, T) \quad (3)$$

and

$$|B| = \frac{1}{6} x N_0 \beta s_0(x) B_J(\mathbf{B}, x, T), \quad (4)$$

where  $N_0\alpha$  and  $N_0\beta$  are 220 and 880 meV,<sup>15</sup> respectively and  $s_0(x)$ , the effective spin of the manganese ions, is a function of  $x$ , which accounts for the antiferromagnetic coupling between the manganese ions.<sup>16</sup>  $B_J(\mathbf{B}, x, T)$  is a modified Brillouin function that depends upon the external magnetic field  $\mathbf{B}$ , the manganese concentration  $x$ , and the temperature  $T$ .

Electronic transitions associated with the  $\sigma^-$  polarization observe an increase in the apparent band gap of  $|3A| + |3B|$ , whereas those associated with the  $\sigma^+$  optical polarization observe a decrease in the band gap of  $|3A| + |3B|$ . The changes in the conduction-band potential  $3A$  and the valence-band potential  $3B$  are nonlinear functions of the magnetic field. This feature, coupled with the variation in alloy composition, produces highly nonlinear conduction- and valence-band responses in an external magnetic field. This is illustrated in Fig. 3. The graph displays the valence-band potential profile for a 150/150 Å single sawtooth period. In the absence of an external magnetic field (0

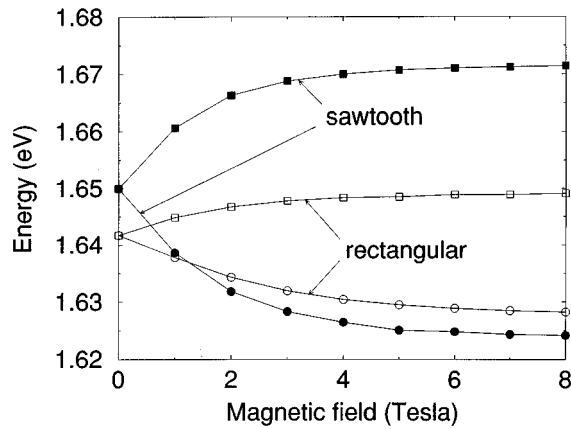


FIG. 4. Comparison of the magnetic-field splittings of the  $\sigma^-$  (upper branches) and  $\sigma^+$  (lower branches) of the sawtooth and rectangular superlattices.

T) the potential profile is proportional to the alloy composition  $x$ , as in the earlier work cited previously.<sup>1-4</sup> However, upon the application of a magnetic field  $\mathbf{B}$  the nonlinear response of the valence-band edge across the well produces the potential profile shown for fields of 1, 3, and 8 T. Similar profiles are obtained for the conduction band, but the effect is much less marked. It is to be noted that, in contrast with nonmagnetic semiconductors, the direct effect of the magnetic field on the form of the potential in the  $z$  direction has a much more pronounced influence on the exciton energies than does the lateral (parabolic) confining potential due to the magnetic field.

The effect of the magnetic field on the heavy-hole exciton energy at 1.8 K is illustrated in Fig. 4. The figure compares the magnetic-field splittings (upper branches correspond to  $\sigma^-$  and lower to  $\sigma^+$  polarizations) of a 5 period 40/40 Å sawtooth with the standard rectangular Kronig-Penney superlattice of the same period. The average manganese concentrations of both systems are identical and equal to 0.0375.

The point of interest is the significant enhancement of the magnetic field splitting of the sawtooth superlattice over the comparable rectangular superlattice structure. The splitting is almost 50 meV compared with 20 meV in the rectangular superlattice.

Figure 4 demonstrates one advantage of the magnetic sawtooth superlattice over the equivalent rectangular superlattice as far as the tunability of the emission energy via an external magnetic field is concerned. An optical device constructed from a dilute magnetic semiconductor superlattice would have a magnetic field tunability of the photoluminescence emission (lowest-energy transition) of around 14 meV if the superlattice modulation were of the standard rectangular type. However, this could be increased to 26 meV by using a sawtooth profile.

Figure 5 displays the exciton binding energies corresponding to the total energies of Fig. 4. The changes in the binding energies as a function of magnetic field are  $\sim 1$  meV for the rectangular profile, and are considerably less for the sawtooth superlattice. Exciton binding energy changes of this magnitude have been observed previously by Jackson *et al.*<sup>8</sup> for rectangular superlattices. This same work<sup>8</sup> also reported constant relative oscillator strengths of the exciton

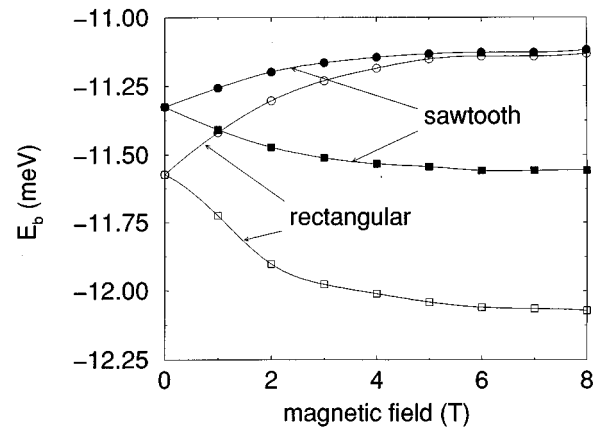


FIG. 5. Comparison of the exciton binding energies as a function of magnetic field of the  $\sigma^-$  (lower branches, higher absolute binding energy) and  $\sigma^+$  (higher branches, lower binding energy) of the sawtooth and rectangular superlattices.

transitions as a function of field. The calculations described here indicate small changes of around 10%, which would be difficult to detect in a photoluminescence experiment.

Figure 6 displays the temperature dependence of the magnetic-field tunability (energy shift of photoluminescence between 0 and 8 T) of the sawtooth superlattice of Fig. 4. It can be seen that as the temperature increases the tunability of the photoluminescence emission is greatly reduced. This is due to the reduction in the paramagnetism of the  $\text{Cd}_{1-x}\text{Mn}_x\text{Te}$  alloy, a similar dependence is obtained for the standard rectangular superlattice, however, the initial magnitude is of course significantly reduced.

#### IV. CONCLUSION

The effect of an external magnetic field on the exciton energies in a dilute magnetic semiconductor sawtooth superlattice have been presented. These systems have been shown

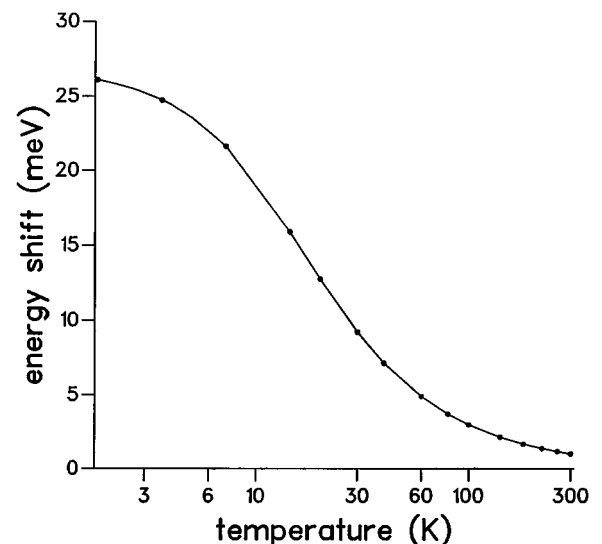


FIG. 6. Temperature dependence of the photoluminescence emission energy shift between 0 and 8 T for a 5 period 40/40 Å sawtooth superlattice.

to exhibit novel band potential profiles under the influence of external magnetic fields. Furthermore, it has been demonstrated that the magnetic tunability of the photoluminescence emission energy of a superlattice can be significantly enhanced by the use of a sawtooth modulation of magnetic ions rather than the standard rectangular modulation.

Recently we have shown<sup>17</sup> that alloy clustering can reduce significantly the magnitude of the Zeeman splitting of exciton lines. It is clear therefore, that if such clustering occurred in a sawtooth superlattice the observed Zeeman split-

ting would be reduced markedly. Hence sawtooth structures could be utilized to probe the occurrence and magnitude of alloy clustering in diluted magnetic semiconductor structures.

#### ACKNOWLEDGMENTS

The authors would like to thank EPSRC (U.K.), the University of Hull, and the University of Leeds for financial support.

\*Electronic address: p.harrison@elec-eng.leeds.ac.uk

<sup>1</sup>F. Capasso, S. Luryi, W. T. Tsang, C. G. Bethea, and B. F. Levine, *Phys. Rev. Lett.* **51**, 2318 (1983).

<sup>2</sup>M. Jaros, K. B. Wong, and M. A. Gell, *Phys. Rev. B* **31**, 1205 (1985).

<sup>3</sup>J. A. Brum, P. Voisin, and G. Bastard, *Phys. Rev. B* **33**, 1063 (1986).

<sup>4</sup>V. Milanović, Z. Ikonić, and D. Tjapkin, *Phys. Rev. B* **36**, 8155 (1987).

<sup>5</sup>G. A. Bastard, *Wave Mechanics Applied to Heterostructures* (Editions de Physique, Paris, 1988).

<sup>6</sup>A. Twadoski, M. Nawrochi, and J. Ginter, *Phys. Status Solidi B* **96**, 497 (1979).

<sup>7</sup>J. P. Killingbeck, *Microcomputer Algorithms* (Adam Hilger, Bristol, 1992).

<sup>8</sup>S. R. Jackson, J. E. Nicholls, W. E. Hagston, P. Harrison, T. Stirner, J. H. C. Hogg, B. Lunn, and D. E. Ashenford, *Phys. Rev. B* **50**, 5392 (1994).

<sup>9</sup>P. Harrison, T. Stirner, S. J. Weston, S. R. Bardorf, S. Jackson, W.

E. Hagston, J. H. C. Hogg, J. E. Nicholls, and M. O'Neill, *Phys. Rev. B* **51**, 5477 (1995).

<sup>10</sup>C. P. Hilton, W. E. Hagston, and J. E. Nicholls, *J. Phys. A* **25**, 2395 (1992).

<sup>11</sup>C. P. Hilton, J. Goodwin, P. Harrison, and W. E. Hagston, *J. Phys. A* **25**, 5365 (1992).

<sup>12</sup>J. Warnock, B. T. Jonker, A. Petrou, W. C. Chou, and X. Liu, *Phys. Rev. B* **48**, 17 321 (1993).

<sup>13</sup>T. Piorek, W. E. Hagston, and P. Harrison, *Phys. Rev. B* **52**, 14 111 (1995).

<sup>14</sup>*Semiconductors and Semimetals*, edited by J. K. Furdyna and J. Kossut (Academic, Boston, 1988), Vol. 25.

<sup>15</sup>J. A. Gaj, R. Planel, and G. Fishman, *Solid State Commun.* **29**, 435 (1979).

<sup>16</sup>J. A. Gaj, C. Bodin-Deshayes, P. Peyla, J. Cibert, G. Feuillet, Y. Merle d'Aubigne, R. Romestain, and A. Wasiela, *Proceedings of the 21st International Conference on the Physics of Semiconductors* (World Scientific, Singapore, 1992), p. 1936.

<sup>17</sup>P. Harrison, J. M. Fatah, T. Stirner, and W. E. Hagston, *J. Appl. Phys.* **79**, 1684 (1996).